J Sol-Gel Sci Technol (2017) 82:611–619
DOI 10.1007/s10971-017-4321-3

ORIGINAL PAPER: SOL-GEL, HYBRIDS AND SOLUTION CHEMISTRIES

Sol–gel synthesis and characterization of two-component systems based on MgO

Aleksey A. Vedyagin[1,2] · Ilya V. Mishakov[1,2] · Timofey M. Karnaukhov[1,3] · Elena F. Krivoshapkina[4,5] · Ekaterina V. Ilyina[1] · Tatyana A. Maksimova[1] · Svetlana V. Cherepanova[1] · Pavel V. Krivoshapkin[4,5]

Received: 19 August 2016 / Accepted: 24 January 2017 / Published online: 10 February 2017

Abstract A series of two-component MO_x–MgO systems, where *M* is Cu, Ni, Co, Fe, Mo or W, was synthesized by sol–gel technique. Aqueous solution of inorganic salt-precursor was used as a hydrolyzing agent. Initial xerogels and final oxides were characterized using X-ray diffraction analysis, scanning electron microscopy and low-temperature nitrogen adsorption. Decomposition of xerogels was studied by differential thermal analysis. According to X-ray diffraction analysis, all xerogel samples are characterized with turbostratic structures regardless of nature of the second component. At the same time, presence of inorganic salt in magnesium hydroxide matrix shifts the temperature of decomposition of latter towards lower values. Structural and textural characteristics of MgO-based oxide systems were found to be strongly affected by the additive. Formation of joint phase was observed in the case of cobalt oxide. In most cases, additives turned out to be even distributed in the bulk of MgO, except for WO_3. This oxide formed large agglomerates because of low solubility of precursor.

Graphical Abstract

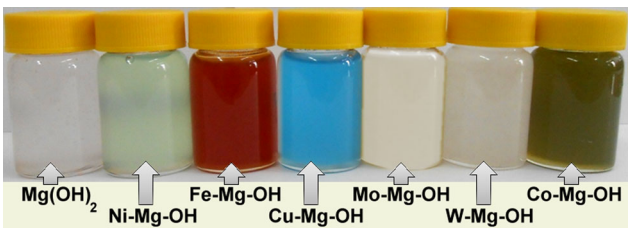

Keywords Sol–gel synthesis · MgO · Two-component oxide systems · Characterization

1 Introduction

Nowadays nanostructured oxide materials attract much attention due to its unique properties, which opens new horizons and widens areas of its application [1, 2]. Such nano-oxides are known to be efficiently used as antibacterial agents, adsorbents, catalysts, and destructive sorbents of toxic chemicals [3]. Among this class of materials, MgO being characterized by an abundance of low-coordinated surface sites occupies a special place [4]. Recently we have shown that both catalytic activity and reactivity of pristine magnesium oxide can be significantly improved by doping with other oxides (VO_x, CoO, etc.) [5–7]. From the other hand, MgO by itself is known to affect the properties of second component. Thus, reducibility of metal oxides can be noticeably changed by strong interaction with MgO lattice [8]. It allows one to consider MgO-based multi-component

Electronic supplementary material The online version of this article (doi:10.1007/s10971-017-4321-3) contains supplementary material, which is available to authorized users.

✉ Aleksey A. Vedyagin
vedyagin@catalysis.ru

[1] Boreskov Institute of Catalysis SB RAS, Novosibirsk 630090, Russia

[2] National Research Tomsk Polytechnic University, Tomsk 634050, Russia

[3] Novosibirsk State University, Novosibirsk 630090, Russia

[4] Institute of Chemistry of Komi SC UB RAS, Syktyvkar 167982, Russia

[5] ITMO University, St. Petersburg 197101, Russia

systems as a hydrogen acceptor with controllable hydrogen uptake within desired temperature region.

In order to obtain multi-component oxide systems, the methods of deposition including impregnation are usually used as the simplest and fastest ones [9–15]. Incipient wetness impregnation provides accurate loading of depositing component while its distribution in a bulk of the support is not uniform. It stipulates the tendency to sintering of these systems especially in locations enriched with second component. Impregnation with excess solution, in its turn, allows one to distribute the additive in the support evenly. Disadvantageously, it requires large volume of impregnating solution, thus increasing the losses of second component. Relatively low dispersity of supporting component is another disadvantage attributed to the most deposition methods.

The alternative methods to prepare multi-component oxide systems include thermal or thermo–chemical approaches where high-temperature sintering and alloying procedures play a key role [16–19]. At the same time, high temperatures are known to facilitate solid state interactions followed by formation of joint phase products. However, appearance of joint phases as usual worsens the reducibility of oxides. It is obvious also, that high temperature synthesis results in a product with high degree of agglomeration and low surface area which whittles away the nanostructural effects.

Another class of preparation methods, co-precipitation, deals with versatile and relatively simple synthetic routes [19–30]. Both chemical and phase composition can be easily varied using this approach. Nevertheless, such aggressive reagents as strong acids and bases are implied to be used in preparation procedures. Additionally, the process of preparation involves formation of harmful wastes in a large amount. Intensive interaction between components which can take place starting from the stage of solution preparation and results in appearance of joint phases should be mentioned as well.

Contrary to the approaches described above, sol–gel technology is considered as the most attractive way to prepare multi-component oxide system with desired properties and satisfying the requirements. Wide controllability of the sol–gel process provides obtaining of oxide composites with preferred chemical composition, textural and structural properties. Being consisted of nanosized particles, these materials, as usual, are characterized by developed surface area and large values of pore volume. From the other hand, sol–gel method is believed to simplify the technological realization of materials preparation process, since most of the stages can be carried out in one reactor. Shaping of the final products into powders, fibers, thin films, granules and monoliths is regarded as an ease task in the most cases.

A variety of sol–gel approaches for synthesis of multi-component oxide systems based on MgO is described in literature. Thus, in [9] sol–gel method was used to obtain precursor of second component which was deposited on crystalline magnesium oxide resulting in formation of NiO–MgO system. Sharma et al. [20] reported about sol–gel preparation of MgO followed by slurrying in diphenyl ether with subsequent deposition on cobalt oxide. In reference [31], organic precursor of second component (iron ethylate) was synthesized and then hydrolyzed simultaneously with magnesium methoxide. In our recent works [6, 32] we have used similar approach when organic precursor of additive was added to freshly prepared magnesium hydroxide gel (in accordance with [33]), and then two-component system was turned into oxide by drying and calcination.

All examples mentioned above can be unified by using organic precursors of components of target oxide systems. However, if obtaining such precursors for magnesium and some other metals does not appear to be a problem, then for the most metals it does. In addition, inorganic salts, which are known to be more available precursors, are poorly dissolve in different organic solvents. As a consequence, it requires development of more complicated, as a rule multistage and exotic methods of preparation of organic compounds containing one or other metal. Besides the additional technological difficulties, complication of synthetic schemes leads to increased residual content of carbon-containing substances in the final oxide product.

In present work, we have applied sol–gel approach to synthesize two-component systems based on MgO. An aqueous solution of inorganic precursors was used instead of distilled water in order to hydrolyze magnesium methoxide. Obtained xerogels and oxides were studied by a set of physicochemical methods that include X-ray diffraction (XRD) analysis, scanning electron microscopy and low-temperature nitrogen adsorption.

2 Experimental

2.1 Preparation of the samples

Pristine MgO was prepared by sol–gel method according to scheme presented in Fig. 1. A sample of magnesium metal ribbon (Aldrich, USA, 99.9 %, 0.15 mm) was cut onto small pieces and blended with dry methanol. Then, toluene was added as a gel stabilizer. Methanol to toluene volume ratio was 1:1. The obtained magnesium methoxide was hydrolyzed dropwise by distilled water at room temperature during 1 h. As a result, fairly stable $Mg(OH)_2$ gel was formed. The gel was dried at room temperature during 2 h, and at 200 °C during another 2 h. In order to obtain MgO,

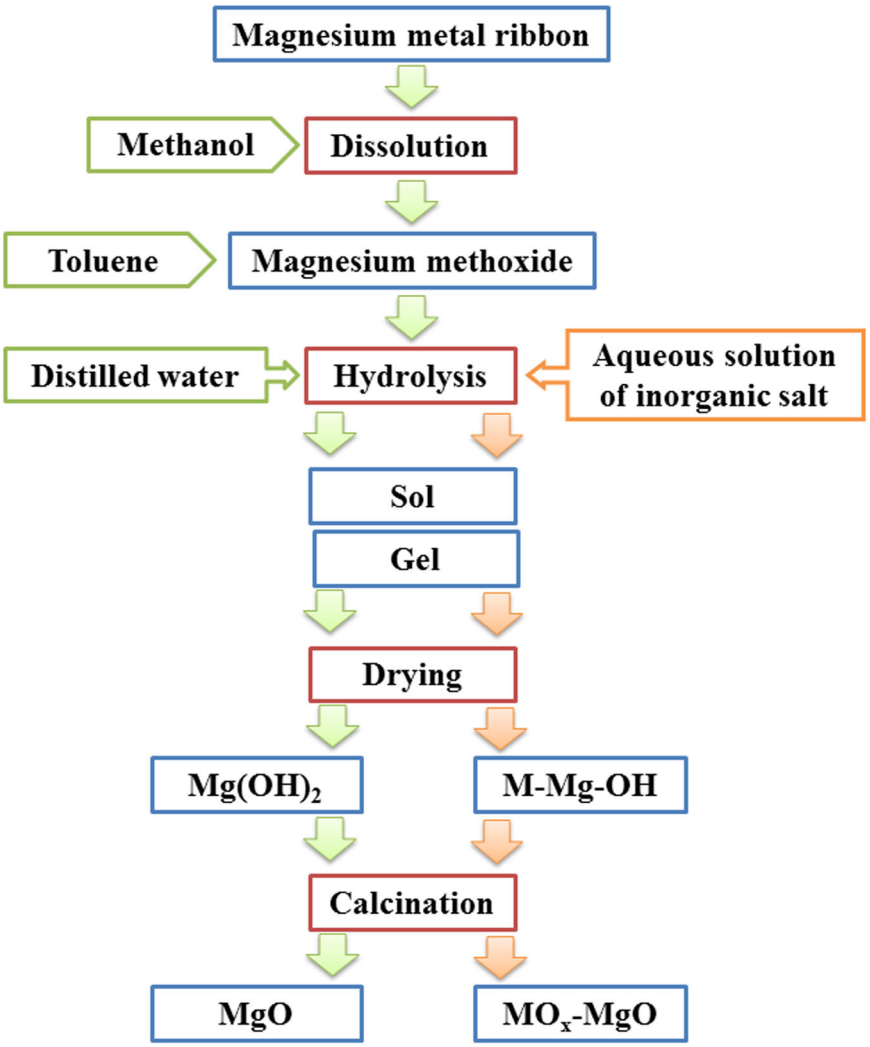

Fig. 1 Scheme of MgO and MO_x-MgO synthesis

xerogel was calcined stepwise as follows: heating up from room temperature to 300 °C with ramping rate of 5 °C/min, heating up to 400 °C with ramping rate of 1 °C/min, and, finally, heating up to 500 °C with ramping rate of 5 °C/min.

MO_x-MgO systems (where *M* is Cu, Ni, Co, Fe, Mo or W) were prepared analogously (Fig. 1). Aqueous solution of corresponding inorganic salts was used as a hydrolyzing agent instead of distilled water. Inorganic precursors used in this research and chemical composition of final composites are listed in Table 1. The concentration of second component in all cases was 15 wt.% in regard to corresponding oxide.

Table 1 Inorganic precursors used in this work and chemical composition of resulting two-component oxide systems

#	Sample	Inorganic precursor	Chemical composition of oxide systems
1	W–Mg–O	$(NH_4)_{10}(W_{12}O_{41})\cdot 5H_2O$	WO_3–MgO
2	Fe–Mg–O	$Fe(NO_3)_3\bullet 6H_2O$	Fe_2O_3–MgO
3	Mo–Mg–O	$(NH_4)_6Mo_7O_{24}\bullet 4H_2O$	MoO_3–MgO
4	Co–Mg–O	$Co(NO_3)_2\bullet 6H_2O$	Co_3O_4–MgO
5	Ni–Mg–O	$Ni(NO_3)_2\bullet 6H_2O$	NiO–MgO
6	Cu–Mg–O	$Cu(NO_3)_2\bullet 3H_2O$	CuO–MgO

2.2 Characterization of the samples

In order to select the temperature profile for calcination procedure, the xerogel samples were investigated by differential thermal analysis (DTA). DTA curves were recorded on a Netzsch STA 409 PC/PG device in the temperature range of 25–700 °C. The heating rate of the samples was 5 °C/min.

The specific surface areas (SSA) of the synthesized samples were measured using low-temperature nitrogen adsorption. The pore size distributions were determined from the nitrogen adsorption isotherms at 77 K using

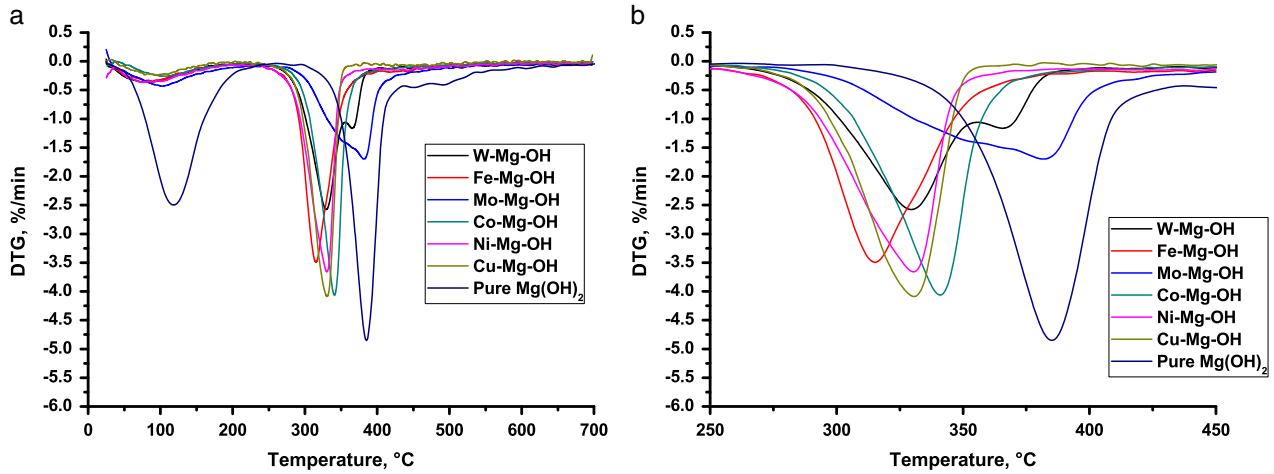

Fig. 2 DTA of pure magnesium hydroxide and two-component xerogels M–Mg–OH

ASAP-2400 (Micrometrics, USA) and Digisorb–2600 instruments (Quantochrome, USA).

The XRD patterns of the samples were acquired using a X'TRA (Thermo ARL, Switzerland) diffractometer operating with a CuKa radiation source (k = 1.5418 A) in the 2 h angle range 5–85° with 5 s accumulation in each point. Lattice constants for all compounds were refined using TOPAS software (Bruker, Germany). The average crystallite sizes were calculated using the Scherrer equation.

The morphology and structure of the xerogel and oxide samples were studied using a JSM-6460 (Jeol, Japan) scanning electron microscope. The microscope ensured magnifications from ×8 to ×300,000.

3 Results and discussion

3.1 Simplification of preparative procedure

As it was already mentioned, sol–gel approaches to synthesis of multi-component oxide systems described in literature implicate using of organic precursors, thus complicating the synthetic method and increasing the residual content of organic substances in final product. In present work, we have modified the traditional procedure and refused to use alkoxide precursors of second component. Whereas during the synthesis, water is needed as hydrolyzing agent; we have decided to prepare aqueous solutions containing required amount of corresponding salts, and used it instead of water while hydrolyzing magnesium methoxide.

It should be noted that this simplified approach has one serious disadvantage. Presence of a salt in the moment when colloidal system is being formed destabilizes forming particles, facilitates its agglomeration (coagulation) and, thus, leads to worsening of textural characteristics of the oxides being prepared. The most probable reason of it is a rise of acidity of the precursor's aqueous solution which takes place due to hydrolysis of metal cation in the hydration shell.

Here, we had not intentionally tried to affect the stability of obtaining colloids with an aim to keep the preparation conditions the same and to compare the characteristics of final products. At the same time, an increase of volume of the gel stabilizing agent (toluene) as well as pH control on the stage of colloid formation by preliminary addition of reagents facilitating mild decrease of acidity (epoxides, as example) are known to enhance the stability of colloidal particles. All these tricks will be used on the next stages of the study.

3.2 Study on decomposition of *M*–Mg–O xerogels

Figure 2a shows thermogravimetric curves for pure Mg $(OH)_2$ and *M*–Mg–O xerogels. Two temperature regions should be taken into consideration. The first one, from room temperature to near 200 °C, is attributed to removal of adsorbed (weakly bonded) water. The second region is presented in Fig. 2b for more evidence. It is seen, that corresponding peak for pure magnesium hydroxide is significantly larger if compare with two-component samples. The main peak assigned to decomposition of hydroxide has a maximum at 386 °C (Table 2). The process of decomposition ends almost completely at about 500 °C. It is obvious that introduction of second component leads to a shift of the main peak towards lower temperatures. In the case of iron-containing system the peak is shifted on a maximum value of 76 °C. At the same time, W-Mg-OH and Mo-Mg-OH samples are characterized with widening and splitting of main peak, which means that at least two steps

Table 2 Second temperature interval of weight loss for pure magnesium hydroxide and two-component M-Mg-OH xerogels according to DTA

Sample	Temperature interval of weight loss (°C)	Main peak position (°C)
$Mg(OH)_2$	300–440	386
W–Mg–OH	270–390	330, 367
Fe–Mg–OH	260–380	310
Mo–Mg–OH	270–440	370, 385
Co–Mg–OH	260–390	342
Ni–Mg–OH	250–370	331
Cu–Mg–OH	260–360	331

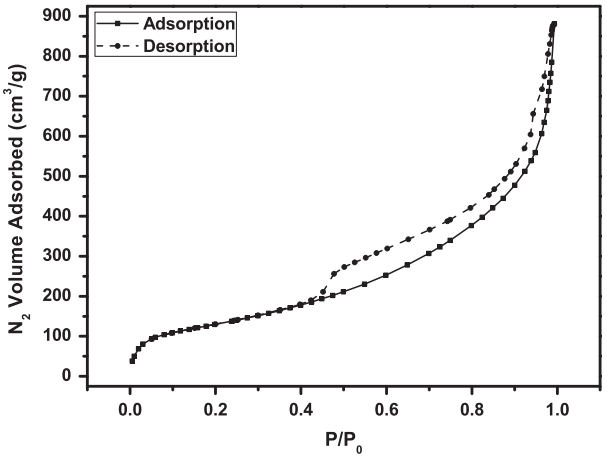

Fig. 3 Type IV isotherm of Mo–Mg–OH xerogel sample

Table 3 Textural properties of M–Mg–OH in accordance with low-temperature nitrogen adsorption

Sample	*SSA* (m^2/r)	V_{pore} (cm^3/g)	D_{av} (Å)
W–Mg–OH	564	1.58	112
Fe–Mg–OH	269	1.00	149
Mo–Mg–OH	475	1.36	114
Co–Mg–OH	235	0.40	67
Ni–Mg–OH	465	0.92	79
Cu–Mg–OH	406	1.20	118

of dehydration and salt-precursor decomposition are present. Note that in these cases, inorganic precursors used were different from those for other metals. In other cases decomposition of metal nitrate is believed to occur simultaneously with dehydration process.

The observed shift of main decomposition peak toward low-temperature area can be explained as follows. It is known that intercalation of salt into interlayer space of magnesium hydroxide increases distance between layers and, correspondingly, its pore sizes [34]. It eases the dehydration process and leads to reduction of decomposition temperature. Additionally, the process of precursor decomposition itself can affect positively on dehydration process by loosening the hydroxide matrix.

It can be concluded here that the calcination temperature of 500 °C is enough for both complete dehydration of hydroxide and decomposition of inorganic salts used.

3.3 Characterization of *M*–Mg–OH xerogels

All prepared *M*–Mg–OH xerogels were characterized by low-temperature nitrogen adsorption. Corresponding isotherms are presented in Fig. 3 and Supplementary Fig. S1. It is seen that all isotherms are of type IV with hysteresis loops caused by capillary condensation taking place in micro/mesopores. Calculated values of specific surface area, pore volume and average pore diameter are summarized in Table 3. In general, samples synthesized by sol–gel method are characterized by developed surface area (above 200 m^2/g) and large values of pore volume. Addition of second component decreases surface area of xerogels. This effect is heavily represented in the case of iron and cobalt when SSA reduces in 2.5 times and higher. Note that surface area of pure $Mg(OH)_2$ was as high as 680 m^2/g. The minimal effect was observed for W-Mg-OH sample. It is also seen that an increase of average pore diameter (D_{av}) occurs in all cases. The maximum value of D_{av} (149 Å) was found for the Fe-Mg-O sample. At the same time, the smallest average pore diameter (67 Å) achieved for Co-Mg-O explains the difference in the form of hysteresis loop in isotherm of this sample (Supplementary Fig. S1c).

According to results of XRD analysis shown in Fig. 4, all *M*-Mg-O samples are very similar to each other. XRD patterns for the samples correspond to layered disordered (turbostratic) structure which is specified mostly by magnesium hydroxide. Appearance of the turbostratic structure for the systems based on $Mg(OH)_2$ was approved in our recent work [35]. No other phases were detected. Size of coherent-scattering regions (CSR) of crystallites is of few nanometers for all samples of the series. A considerable expansion of interlayer distance (d_{001}) comparing with brucite (4.77 Å) was observed in all cases. Numerical data of XRD analysis are presented in Table 4. Average sizes of CSR for perpendicular and parallel layers are labeled as $D_{\perp}$ and $D_{\parallel}$ accordingly.

As it was reported earlier [35], expansion of interlayer distance in the case of systems prepared using sol–gel approach is connected with incorporation of methanol molecules between the magnesium hydroxide layers. It should be noted that even larger expansion of d_{001} was observed for two-component systems in the present study.

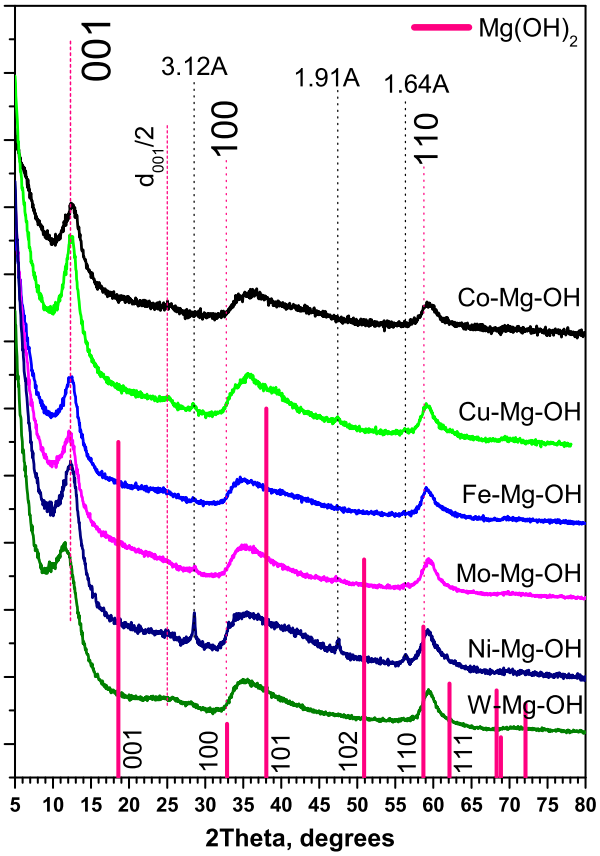

Fig. 4 XRD patterns for M–Mg–OH xerogel samples

Table 4 XRD data for M–Mg–OH xerogel samples

Sample	d_{001} (Å)	$D_{\perp}$ (nm)	$D_{\parallel}$ (nm)
W–Mg–OH	7.58	3.7	5.8
Fe–Mg–OH	7.17	5.3	5.7
Mo–Mg–OH	7.24	5.3	5.5
Co–Mg–OH	7.03	4.1	4.8
Ni–Mg–OH	7.16	4.8	4.6
Cu–Mg–OH	7.14	5.2	5.2

Most probably, anions of salt-precursor of second component in addition to methanol are incorporated into interlayer space of magnesium hydroxide matrix.

The xerogel samples were studied by scanning electron microscopy. As an example, SEM image for Mo–Mg–OH is shown in Fig. 5a. Corresponding images for other samples of this series are presented in Supplementary Fig. S2. No evident differences in terms of morphology were observed. All systems are represented by disordered layered agglomerates of few microns in size.

Thus, it can be concluded that introduction of second component in the form of salt-precursor has very poor effect on morphological structure of the xerogels. At the same time, it noticeably modifies textural and structural properties of magnesium hydroxide in relation to the nature of additives. The value of surface area decreases in a row: W–Mg–OH > Mo–Mg–OH > Ni–Mg–OH > Cu–Mg–OH > Fe–Mg–OH > Co–Mg–OH. Interlayer distance changes in a following order: W–Mg–OH > Mo–Mg–OH > Fe–Mg–OH > Ni–Mg–OH > Cu–Mg–OH > Co–Mg–OH. It is obvious that tungsten-containing sample occupies leading positions on these parameters. As it was already mentioned, precursor of this metal has low solubility which means that it is contained in hydroxide matrix in a form of small particles or even agglomerates. The mechanism of intercalation changes in this case, thus resulting in increased interlayer distance and highest surface area.

3.4 Characterization of the oxides MO_x–MgO

Figure 5b and Supplementary Fig. S3 illustrate SEM images of two-component systems after being calcined at 500 °C according to temperature profile described above. As seen, all oxide samples are represented by microsized agglomerates of small plates (crystallites). No noticeable features were found using this characterization technique.

Nitrogen adsorption isotherms are presented in Fig. 6 and Supplementary Fig. S4. Character of isotherms is very similar for all samples. Table 5 summarizes the textural characteristics of two-component oxides. As it follows, surface area of the samples after calcination procedure is significantly lower if compare with xerogels. The highest value (342 m^2/g) was observed for Mo–Mg–O sample, while the lowest (113 m^2/g)—for Co–Mg–O. Addition of second component has the same trend in influence on surface area as in the case of xerogels. *SSA* of *M*–Mg–O differs from that of MgO (216 m^2/g) in 1.5–2 times. The only exception was Mo–Mg–O sample which has enhanced surface area. Average pore diameter increases in all cases. Among the studied series, Cu–Mg–O sample was found to have the largest pore size of 331 Å.

Figure 7 shows the results of XRD analysis for *M*–Mg–O samples. Table 6 summarizes the following parameters obtained by XRD: a—lattice parameter of MgO; D_1—average size of CSR for main phase (MgO with intercalated cations of other metal); D_2-average size of CSR for second phase (if present); w_1—weight fraction of main phase. Reflexes corresponding to magnesium oxide can be clearly seen in XRD patterns of all samples. Lattice parameter of MgO is lightly increased regarding to periclase (4.13 Å), which indicates an intercalation of larger cations of second metal into it (see Table 6). Asymmetry of the 111 peak for MgO facilitates towards inclusion of spinel-like fragments into its structure [36]. In some cases, formation of small amount of joint phases was observed. Thus, appearance of $MgCo_2O_4$ phase was detected for Co–Mg–O system. XRD

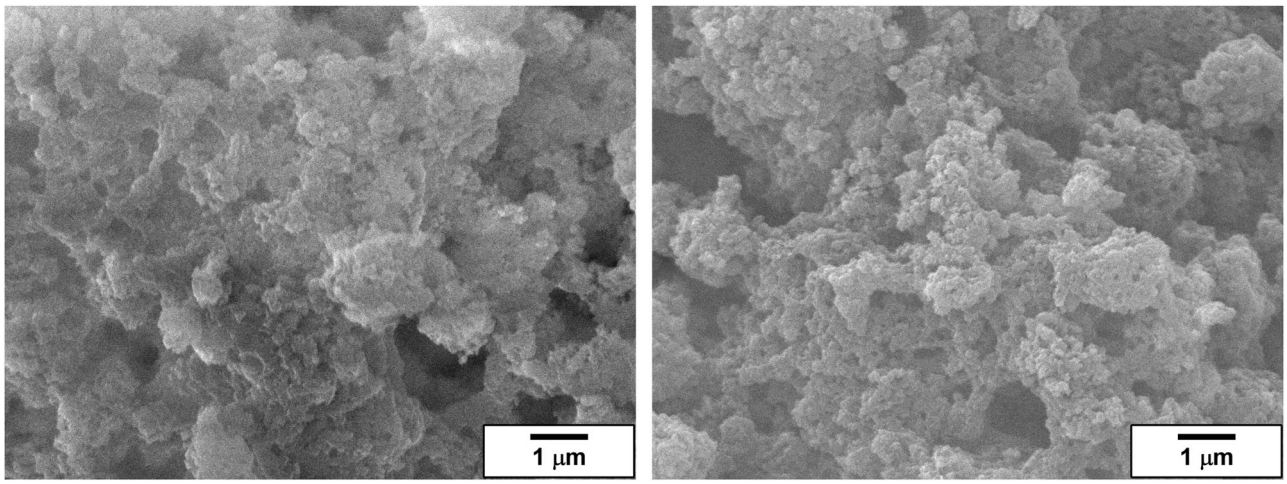

Fig. 5 SEM images for Mo–Mg–OH (**a**) and Mo–Mg–O (**b**) samples

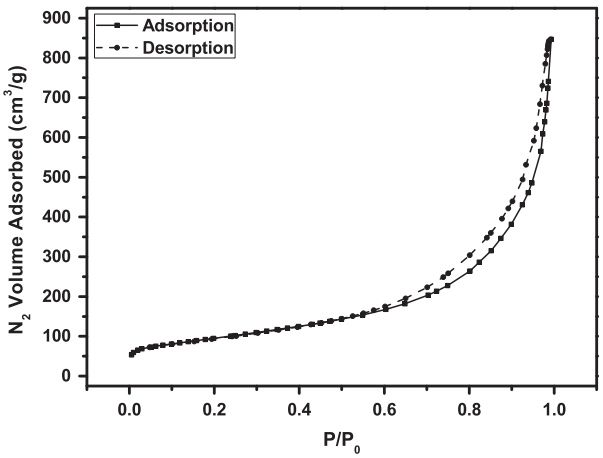

Fig. 6 Type IV isotherm of Mo–Mg–O oxide sample

Table 5 Textural properties of M–Mg–O in accordance with low-temperature nitrogen adsorption

Sample	*SSA* (m^2/r)	V_{pore} (cm^3/g)	D_{av} (Å)
W–Mg–O	212	0.95	180
Fe–Mg–O	120	0.70	233
Mo–Mg–O	342	1.30	153
Co–Mg–O	113	0.64	225
Ni–Mg–O	154	0.72	189
Cu–Mg–O	125	1.03	331

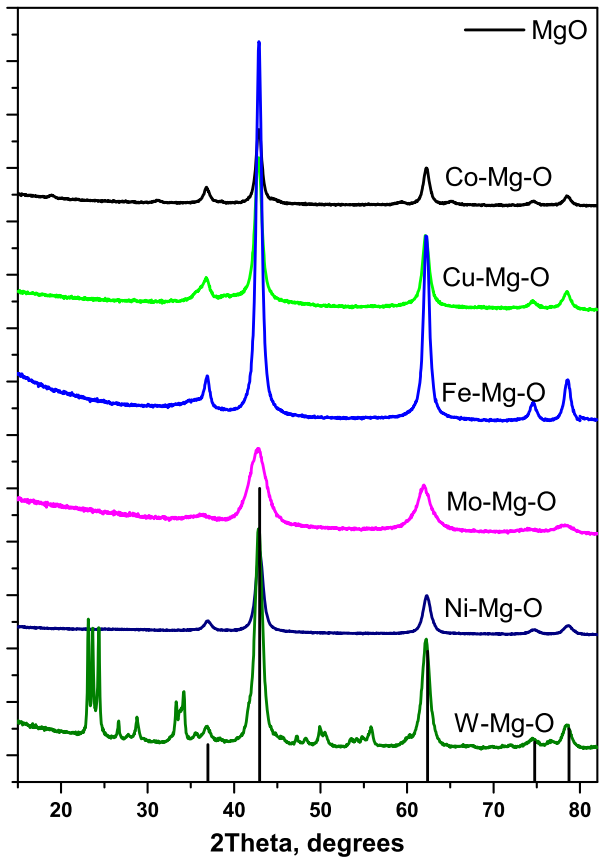

Fig. 7 XRD patterns for M–Mg–O oxide samples

pattern for W-containing samples shows reflexes of tungsten oxide WO_3 in a form of large (about 100 nm) particles. WO_3 is monoclinic (PDF#43-1035, space group $P2_1/n$, $a = 7.297$ Å, $b = 7.539$ Å, $c = 7.688$ Å, $\beta = 90.91°$). Refined lattice constants for tungsten oxide in W-Mg-O are represented in Table 6. This sample clearly shows the limitation of the approach applied, which is connected with poor solubility. Ammonium paratungstate used as a precursor in this case has significantly lower solubility in water if compared with nitrates (Cu, Co, Ni, and Fe) or even

Table 6 XRD data for M–Mg–O oxide samples

Sample	a (Å)	D_1 (nm)	Second phase, D_2 (nm)	w_1 (wt.%)	Lattice parameters of second phase
WO_3–MgO	4.2221	7–9	$WO_3 > 100$	94	$a = 7.312$ Å $b = 7.526$ Å $c = 7.689$ Å $\beta = 90.45^\circ$
Fe_2O_3–MgO	4.2193	9–12	–	100	
MoO_3–MgO	4.2351	3–4	–	100	
Co_3O_4–MgO	4.2187	9–11	$MgCo_2O_4$ 7–10	91	$a = 8.108$ Å
NiO–MgO	4.2141	7–9	–	100	
CuO–MgO	4.2247	7–9	–	100	

ammonium heptamolybdate. Thereby, aqueos solution of ammonium paratungstate being used as a hydrolyzing agent rapidly reaches local oversaturated state. It leads to salt sedimentation occurred prior to its fine distribution in magnesium hydroxide matrix.

4 Conclusions

In present study, a series of hydroxide and oxide Mg-based systems were synthesized by simplified sol–gel method. It was shown that inorganic salt of second component can be used as a precursor instead of traditionally applied metal–organic compounds. The salt can be added in the form of aqueous solution used as a hydrolyzing agent. Water solubility of precursor affects the dispersion and distribution of the second component in the lattice of MgO. Structural and textural properties of both *M*–Mg–OH xerogels and *M*–Mg–O oxides were found to be determined by the nature of intercalant.

Acknowledgements This work has been performed within the state-guaranteed order for Boreskov Institute of Catalysis (project number 0303-2016-0014). DTA experiments were provided using the equipment of Center for Collective Use "Khimiya" (Institute of Chemistry of Komi Scientific Centre UB RAS).

Compliance with ethical standards

Conflict of interest The authors declare that they have no competing interests.

References

1. Hu J, Chen L, Richards R (2008) Properties, synthesis and applications of highly dispersed metal oxide catalysts. In: Jackson SD, Hargreaves JSJ (Eds) Metal oxide catalysis, Wiley-VCH Verlag GmbH & Co. KGaA, Weinheim, Germany
2. Ozin GA, Arsenault AC, Cademartiri L (2009) Nanochemistry: a chemical approach to nanomaterials. Royal Society of Chemistry, London
3. Ilyina EV, Mishakov IV, Vedyagin AA (2009) Preparation of nanocrystalline $VMg(OH)_x$ and VOx·MgO from organometallic precursors. Inorg Mater 45:1267–1270
4. Klabunde KJ, Stark J, Koper O, Mohs C, Park DG, Decker S, Jiang Y, Lagadic I, Zhang D (1996) Nanocrystals as stoichiometric reagents with unique surface chemistry. J Phys Chem 100:12142–12153
5. Ilyina EV, Mishakov IV, Vedyagin AA, Bedilo AF, Klabunde KJ (2013) Promoting effect of vanadium on CF_2Cl_2 destructive sorption over nanocrystalline mesoporous MgO. Microporous Mesoporous Mater 175:76–84
6. Ilyina EV, Mishakov IV, Vedyagin AA, Bedilo AF (2013) Aerogel method for preparation of nanocrystalline CoO_x-MgO and VO_x-MgO catalysts. J Solgel Sci Technol 68:423–428
7. Bedilo AF, Shuvarakova EI, Volodin AM, Ilyina EV, Mishakov IV, Vedyagin AA, Chesnokov VV, Heroux DS, Klabunde KJ (2014) Effect of modification with vanadium or carbon on destructive sorption of halocarbons over nanocrystalline MgO: The role of active sites in initiation of the solid-state reaction. J Phys Chem C 118:13715–13725
8. Parmaliana A, Arena F, Frusteri F, Giordano N (1990) Temperature-programmed reduction study of NiO–MgO interactions in magnesia-supported Ni catalysts and NiO–MgO physical mixture. J Chem Soc Faraday Trans 86:2663–2669
9. Kokubun Y, Amano Y, Meguro Y, Nakagomi S (2016) NiO films grown epitaxially on MgO substrates by sol–gel method. Thin Solid Films 601:76–79
10. Delmon B (1997) Formation of final catalyst. In: Ertl G Knozinger H, Weitkamp J (Eds) Handbook of Heterogeneous Catalysis, Vol 3. Wiley–VCH, Weinheeim
11. Martin C, Rives V, Solana G (1996) Adsorption and oxidation of propan-2-ol on WO_3/MgO. React Kinet Catal Lett 58:243–248
12. Hasegawa S, Tanaka T, Kudo M, Mamada H, Hattori H, Yoshida S (1992) Structure and reactivity of MoO_3-MgO catalyst. Catal Lett 12:255–266
13. Bare SR (1998) Surface Structure of Highly Dispersed MoO_3 on MgO Using in Situ Mo L_3-Edge XANES. Langmuir 14:1500–1504
14. Klicpera T, Zdrăzil M (1999) High surface area MoO_3/MgO: preparation by the new slurry impregnation method and activity in sulphided state in hydrodesulphurization of benzothiophene. Catal Lett 58:47–51
15. Zhang W, Tay HL, Lim SS, Wang Y, Zhong Z, Xu R (2010) Supported cobalt oxide on MgO: Highly efficient catalysts for degradation of organic dyes in dilute solutions. Appl Catal B 95:93–99
16. Szczerba J, Prorok R, Stoch P, Śnieżek E, Jastrzębska I (2015) Position of Fe ions in MgO crystalline structure. Nukleonika 60 (1):143–145
17. Flor G, Riccardi R (1976) Kinetics of $MgWO_4$ formation in the solid state reaction between MgO and WO_3. Z Naturforsch 31a:619–621
18. Massarotti V, Flor G, Marini A, Riccardi R (1980) Molybdates solid state synthesis: the MgO—MoO_3 System. Z Naturforsch 35a:500–502
19. Kamioka N, Ichitsubo T, Uda T, Imashuku S, Taninouchi Y, Matsubara E (2008) Synthesis of spinel-type magnesium cobalt oxide and its electrical conductivity. Mater Trans 49:824–828
20. Sharma G, Jeevanandam P (2013) Synthesis of MgO supported Co_3O_4 nanoparticles by a novel thermal decomposition approach and studies on their magnetic properties. Microporous Mesoporous Mater 165:55–62

21. Fattah Z, Rezaei M, Biabani-Ravandi A, Irankhah A (2014) Preparation of Co–MgO mixed oxide nanocatalysts for low temperature CO oxidation: optimization of preparation conditions. Process Saf Environ Prot 92:948–956
22. Darbar D, Reddy MV, Sundarrajan S, Pattabiraman R, Ramakrishna S, Chowdari BVR (2016) Anodic electrochemical performances of $MgCo_2O_4$ synthesized by oxalate decomposition method and electrospinning technique for Li-ion battery application. Mater Res Bull 73:369–376
23. Fattah Z, Rezaei M, Biabani-Ravandi A, Irankhah A, Arandiyan HR (2016) Synthesis, characterization and application of Co–MgO mixed oxides in oxidation of carbon monoxide. Chem Eng Commun 203:200–209
24. Kaviyarasu K, Magdalane CM, Anand K, Manikandan E, Maaza M (2015) Synthesis and characterization studies of MgO:CuO nanocrystals by wet-chemical method. Spectrochim Acta A Mol Biomol Spectrosc 142:405–409
25. Zanganeh R, Rezaei M, Zamaniyan A (2014) Preparation of nanocrystalline NiO–MgO solid solution powders as catalyst for methane reforming with carbon dioxide: effect of preparation conditions. Adv Powder Technol 25:1111–1117
26. Jafarbegloo M, Tarlani A, Mesbah AW, Muzart J, Sahebdelfar S (2016) NiO–MgO solid solution prepared by sol–gel method as precursor for Ni/MgO methane dry reforming catalyst: effect of calcination temperature on catalytic performance. Catal Lett 146:238–248
27. Jafarbegloo M, Tarlani A, Mesbah AW, Sahebdelfar S (2015) One-pot synthesis of NiO-MgO nanocatalysts for CO_2 reforming of methane: the influence of active metal content on catalytic performance. J Nat Gas Sci Eng 27:1165–1173
28. Cai X, Wang H, Zhang Q, Tong J (2014) Selective oxidation of styrene efficiently catalyzed by spinel Mg–Cu ferrite complex oxides in water. J Solgel Sci Technol 69:33–39
29. Azam M, Riaz S, Akbar A, Naseem S (2015) Structural, magnetic and dielectric properties of spinel $MgFe_2O_4$ by sol–gel route. J Solgel Sci Technol 74:340–351
30. Guo L, Zhong Y, Gao J, Yang Z, Guo Z (2015) Influence of coating MgO with coprecipitation method on sticking during fluidized bed reduction of Fe_2O_3 particles. Powder Technol 284:210–217
31. Holec P, Plocek J, Nižňansky D, Vejpravová PJ (2009) Preparation of $MgFe_2O_4$ nanoparticles by microemulsion method and their characterization. J Solgel Sci Technol 51:301–305
32. Mishakov IV, Ilyina EV, Bedilo AF, Vedyagin AA (2009) Nanocrystalline aerogel VO_x/MgO as a catalyst for oxidative dehydrogenation of propane. React Kinet Catal Lett 97: 355–361
33. Utamapanya S, Klabunde KJ, Schlup JR (1991) Nanoscale metal oxide particles/clusters as chemical reagents. Synthesis and properties of ultrahigh surface area magnesium hydroxide and magnesium oxide. Chem Mater 3:175–181
34. Shkatulov A, Aristov Y (2015) Modification of magnesium and calcium hydroxides with salts: An efficient way to advanced materials for storage of middle-temperature heat. Energy 85:667–676
35. Ilyina EV, Mishakov IV, Vedyagin AA, Cherepanova SV, Nadeev AN, Bedilo AF, Klabunde KJ (2012) Synthesis and characterization of mesoporous VO_x/MgO aerogels with high surface area. Microporous Mesoporous Mater 160:32–40
36. Cherepanova SV, Leont'eva NN, Arbuzov AB, Drozdov VA, Belskaya OB, Antonicheva NV (2015) Structure of oxides prepared by decomposition of layered double Mg-Al and Ni-Al hydroxides. J Solid State Chem 225:417–426